SYNTHESIS GAS GENERATION BY CHEMICAL-LOOPING REFORMING IN A CONTINUOUSLY OPERATING LABORATORY REACTOR

Magnus Rydén*, Anders Lyngfelt, Tobias Mattisson
Department of Energy and Environment
Chalmers University of Technology
SE-412 96, Göteborg, Sweden

Abstract

Chemical-looping reforming is a novel reforming technology that can be used for partial oxidation and steam reforming of hydrocarbon fuels. This paper describes continuous chemical-looping reforming of natural gas in a laboratory reactor consisting of two interconnected fluidized beds. Particles composed of 60 wt% NiO and 40 wt% $MgAl_2O_4$ are used as bed material, oxygen carrier and reformer catalyst. There is a continuous circulation of particles between the reactors. In the fuel reactor, the particles are reduced by the fuel, which in turn is partially oxidized to H_2, CO, CO_2 and H_2O. In the air reactor the reduced oxygen carrier is reoxidized with air. Complete conversion of natural gas was achieved and the selectivity towards H_2 and CO was high. In total, 41 hours of reforming were recorded. Formation of solid carbon was noticed for some cases. Adding 25 vol% steam to the natural gas reduced or eliminated the carbon formation.

Keywords: Chemical-looping reforming; hydrogen; synthesis gas.

1. Introduction

The gaseous mixture of H_2 and CO is usually referred to as synthesis gas. It has many uses, for example as feedstock for production of ammonia, methanol and synthetic fuels. Although synthesis gas can be produced from all kinds of fossil fuels, natural gas is the most common feedstock and steam reforming, reaction (1), is the most important method. Partial oxidation, reaction (2), can be used for heavier fuels such as oil or coal while CO_2 reforming, reaction (3), can be used if synthesis gas with extra high CO content is wanted.

Steam reforming: $C_nH_m + nH_2O \rightarrow nCO + (n+½m)H_2$ (1)

*Corresponding author: Tel. (+46) 31 7721457, Email: magnus.ryden@chalmers.se
Fuel 2006; 85: 1631-1641.

Partial oxidation: $C_nH_m + (½n)O_2 \rightarrow nCO + (½m)H_2$ (2)

CO_2 reforming: $C_nH_m + nCO_2 \rightarrow (2n)CO + (½m)H_2$ (3)

Synthesis gas can be used for production of pure H_2 through water-gas shift, reaction (4), followed by a purification step in which H_2 is separated from CO_2 and other impurities.

Water-gas shift: $CO + H_2O \rightarrow CO_2 + H_2$ (4)

The most common methods for H_2 purification are pressure swing adsorption and absorption in amine solvents. Other alternatives, for example membrane separation, show promise but are currently not commercially available.

There are several reasons to believe that H_2 will become more important in the future. There is a steadily increasing H_2 demand for refining, metallurgy and manufacturing of electronic components. In addition to this, H_2 is a carbon free energy carrier. Hence it may have a key role to play in the efforts to reduce anthropogenic greenhouse gas emissions. If H_2 is produced without net release of CO_2, for example from renewable energy sources or from fossil fuels with carbon sequestration, it could be used as a CO_2-free energy carrier in zero-emitting vehicles, highly efficient fuel cells and other environmentally friendly applications.

In this paper, a novel method for production of synthesis gas and H_2 is demonstrated. It is called chemical-looping reforming and has several potential benefits compared to conventional technologies. The outline of the paper is as follows. In section 2, the principles of chemical-looping reforming and an overview of relevant research are presented. In section 3, the test reactor and the experimental procedure are described. In section 4, the results of the experiments are presented and analyzed. In section 5, the results are discussed and further topics of research are suggested.

2. Chemical-looping reforming

Chemical-looping reforming utilizes the same general principles as chemical-looping combustion, which is a novel process concept for heat and power production with inherent CO_2 capture. A basic chemical-looping combustion system has two reactors, one for air and one for fuel, as is illustrated in figure 1.

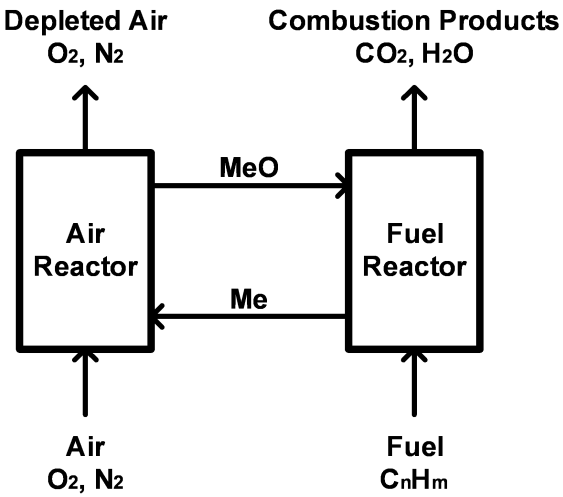

Figure 1. The principles of chemical-looping combustion.

Direct contact between fuel and combustion air is avoided. Instead, an oxygen carrier performs the task of bringing O_2 from the air to the fuel. Thus, the CO_2 produced is not diluted with N_2 and can easily be recovered. In this paper, the abbreviation Me is used to describe a generic oxygen carrier in its reduced form while MeO is used for its oxidized form.

Suitable oxygen carriers are particles of metal oxides such as Fe_2O_3, NiO, CuO or Mn_3O_4. An overview of the research dealing with oxygen-carriers for chemical-looping combustion can be found in the works of Cho [1], Johansson [2] and Adánez et al [3].

Chemical-looping reforming utilizes the same basic principles as chemical-looping combustion. The difference is that the wanted products are not heat but H_2 and CO. Therefore the air to fuel ratio is kept low to prevent the fuel from becoming fully oxidized to CO_2 and H_2O. Chemical-looping reforming in its most basic form could be described as a process for partial oxidation of hydrocarbon fuels where oxygen-carrier particles are used as a source of undiluted oxygen. H_2O or CO_2 can be added to the fuel if steam reforming or CO_2 reforming is wanted in addition to partial oxidation. The basic principles of chemical-looping reforming are illustrated in figure 2.

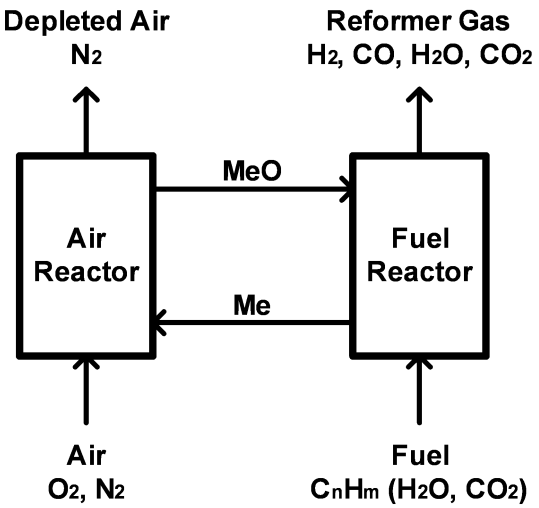

Figure 2. The principles of chemical-looping reforming.

Chemical-looping reforming, as examined in this paper, was originally proposed by Mattissson et al [4]. Similar ideas have also been explored by Stobbe et al [5] and Fathi et al [6]. Oxygen carriers specifically for chemical-looping reforming have been experimentally examined by Zafar et al [7], who performed tests in a fluidized bed reactor with particles of NiO, CuO, Fe_2O_3, and Mn_2O_3, and by Mattisson et al [8]. A process study describing how chemical-looping reforming could be used for large scale cogeneration of H_2 and power has been made by Rydén et al [9].

In a chemical-looping system, the oxygen carrier circulates between the reactors. In the air reactor it is oxidized with O_2 from the combustion air according to reaction (5), and in the fuel reactor it is reduced by the fuel. In chemical-looping combustion the fuel is oxidized to CO_2 and H_2O according to reaction (6). For chemical-looping reforming most of the fuel should undergo partial oxidation, reaction (7), but reaction (6), reaction (1) and reaction (3) could also occur. Steam or CO_2 could be added to the fuel to enhance the relative importance of reaction (1) or reaction (3) respectively.

Me Regeneration: $O_2 + 2Me \rightarrow 2MeO$ (5)

Complete oxidation: $C_nH_m + (2n+\frac{1}{2}m)MeO \rightarrow nCO_2 + (\frac{1}{2}m)H_2O + (2n+\frac{1}{2}m)Me$ (6)

Partial oxidation: $C_nH_m + nMeO \rightarrow nCO + (\frac{1}{2}m)H_2 + nMe$ (7)

The amount of heat released or consumed in the reactor vessels depends on the nature of the oxygen carrier and the fuel, as well as on the reactor temperature. Reaction (5) is strongly exothermic. Reaction (6) is usually endothermic, but exothermic when CuO is used as oxygen carrier. Reaction (1), reaction (3) and reaction (7) are strongly endothermic. If the sum of reactions in the fuel reactor is endothermic, sensible heat needs to be transported from the exothermic air reactor via the oxygen-carrier particles in

order to sustain a suitable reactor temperature. This should always be the case for chemical-looping reforming.

In principle, all kinds of fuels can be utilized in a chemical-looping system. If CH_4 is used as fuel, NiO as oxygen carrier and the reactor temperature is 1200 K, reactions (8-12) occur in the reactor system.

Me Regeneration:	$Ni + ½O_2 \rightarrow NiO$	$\Delta H_{1200} = -234$ kJ/mole	(8)
Complete oxidation:	$CH_4 + 4NiO \rightarrow CO_2 + 2H_2O + 4Ni$	$\Delta H_{1200} = 136$ kJ/mole	(9)
Partial oxidation:	$CH_4 + NiO \rightarrow CO + 2H_2 + Ni$	$\Delta H_{1200} = 211$ kJ/mole	(10)
Steam reforming:	$CH_4 + H_2O \rightarrow CO + 3H_2$	$\Delta H_{1200} = 226$ kJ/mole	(11)
CO_2 reforming:	$CH_4 + CO_2 \rightarrow 2CO + 2H_2$	$\Delta H_{1200} = 259$ kJ/mole	(12)

The exhaust from the air reactor is harmless and consists mainly of N_2. There should be no formation of thermal NO_X since regeneration of the oxygen carrier takes place without flame and at moderate temperature. For chemical-looping combustion, complete oxidation of the fuel is wanted. Consequently, the gas from the fuel reactor should consist of CO_2 and H_2O and the sum of the reactions should be equal to combustion of the fuel with O_2. A condenser is the only equipment needed to obtain pure CO_2 for sequestration.

For chemical-looping reforming, the gas from the fuel reactor should be a mixture consisting of H_2, CO, CO_2 and H_2O. It is also possible that there will be some unreformed fuel. At lower temperatures for instance, full conversion of CH_4 may be hindered by thermodynamical constraints. At atmospheric pressure a fuel reactor temperature in the order of 800 °C is required to obtain 99% conversion of CH_4. At a pressure of 15 bar over 1000 °C is needed. The resulting gas mixture should be similar to what is obtained from conventional fossil fuel reforming and could be used as feedstock for chemical processes, as well as for production of H_2.

Although the same range of oxygen carriers are available for chemical-looping reforming as for chemical-looping combustion, NiO appears more interesting than the alternatives due to its strong catalytic properties. Metallic Ni is used in most commercial steam reforming catalysts. The work of Zafar et al [7] indicated high reaction rate and good selectivity towards H_2 and CO for oxygen carriers with NiO as active phase, while oxygen carriers based on Fe_2O_3, CuO and Mn_2O_3 suffered from poor selectivity and thus produced CO_2, H_2O and unreformed CH_4 rather than CO and H_2.

It should also be mentioned that the thermodynamical properties of CoO indicate that it could be attractive as oxygen carrier for chemical-looping reforming. The possibility to use CoO and CoO/NiO as oxygen-carrier for chemical-looping combustion has been examined by Ishida et al [10], with positive results.

In practice, a chemical-looping process could be designed in several ways, but circulating fluidized beds are likely to have an advantage over other alternatives since this design provides good contact between gas and solids and allows a smooth flow of oxygen carrier between the reactors. In addition to this, circulating fluidized beds are well-known technology that is used for many large scale industrial applications. Chemical-looping combustion using circulating fluidized beds has been successfully demonstrated by Lyngfelt et al [11] and by Ryu et al [12]. Continuous chemical-looping combustion has also been demonstrated by Johansson et al [13] and Abad et al [14], who used the same reactor system as was used for the chemical-looping reforming experiments presented in this paper.

3. Experimental setup

3.1 Laboratory reactor

The experiments were carried out in a laboratory reactor designed for chemical-looping combustion. The reactor is shown in figure 3. For details about the reactor and the cold-flow models upon which the design was based, see Johansson [13] and Kronberger et al [15].

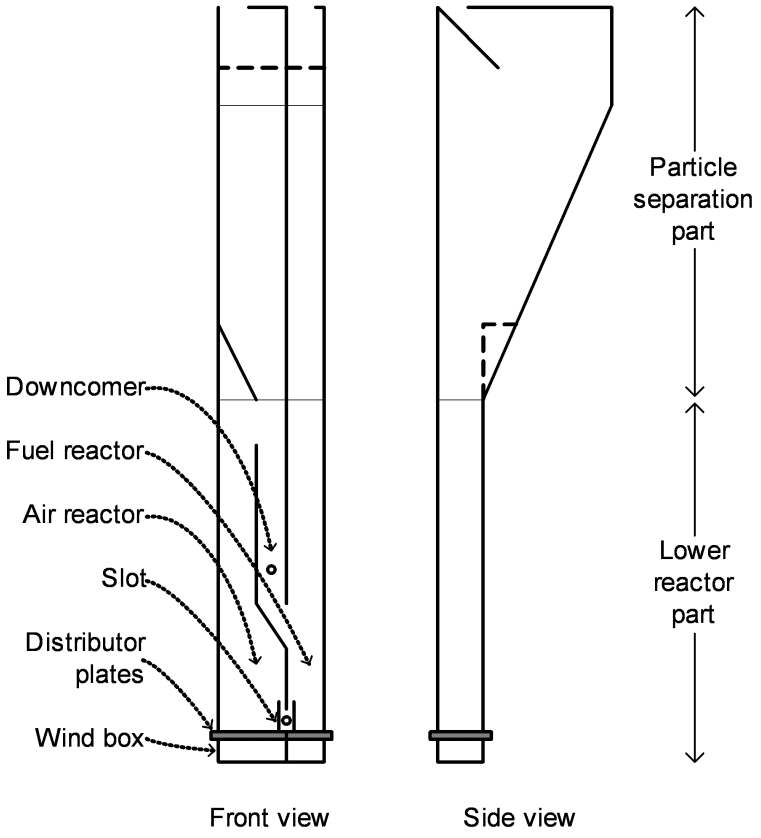

Figure 3. Schematic description of the laboratory reactor.

Fuel and air enter the system through separate wind boxes. Porous quartz plates act as gas distributors. In the air reactor the gas velocity is sufficiently high for oxygen-carrier particles to be thrown upwards, and a fraction of the particles fall into the downcomer, which leads to the fuel reactor. In the downcomer there is a particle column which prevents gas leakage between the reactors. As more particles fall into the downcomer, the column height and the pressure increases and particles are forced into the fuel reactor. This leads to increased bed height and increased pressure in the fuel reactor, which forces particles back into the air reactor through a slot situated in the bottom of the wall between the reactors. In this straightforward manner, a continuous circulation of oxygen-carrier particles is obtained.

The reactor is designed for thermal powers between 100 and 300 W. The base of the fuel reactor measures 25×25 mm. The air reactor is 25×40 mm in the bottom and 25×25 mm in the upper narrow part. The lower reactor part is 200 mm high. Above the lower reactor part there is a separate part for particle separation. Here, the vessel widens to decrease the gas velocity and allow particles to fall back into the reactor beds. The particle separation part is 240 mm high, and in the first 180 mm the reactor depth expands from 25 mm to 105 mm. The last 60 mm has a constant cross-section area. The particles falling down in the sloping section above the air reactor are led to the downcomer by a leaning wall. The downcomer is 117 mm high, has a width of 12 mm and begins 50 mm above the gas distributor plates. The upper part of the opening to the fuel reactor is at a height of 75 mm. Thus, the opening itself is 25 mm.

It is possible to add gas through a hole in the side of the downcomer to fluidize the particle column and thus facilitate the circulation. In the bottom of the reactor, there is a slot that connects the fuel reactor and the air reactor. It has two 15 mm walls rising from the bottom plate, separated by 10 mm. The wall that separates the fuel and air reactor is situated between these two walls and stops 11 mm above the bottom plate. Between the two walls is a horizontal pipe, which has three 1-mm holes directed downwards through which small amounts of fluidizing gas can be injected to improve the circulation.

To make it possible to reach suitable temperatures, the whole reactor is placed inside an electrically heated furnace. The temperature of the furnace is controlled with thermocouples located inside the furnace, just outside the reactor.

3.2 Oxygen-carrier particles

The oxygen-carrier particles used in the experiments were from a batch that originally was used for chemical-looping combustion, see Johansson [13]. The particles were spherical and composed of 60 wt% NiO and 40 wt% $MgAl_2O_4$. They were prepared by freeze granulation and sintered at 1400 °C for 6 hours before they were sieved to 90-212

μm. The particles had a bulk density of 1740 kg/m^3. Similar particles have been examined by Mattisson et al [16], who also gives a detailed description of the production process. In total, 350 g oxygen-carrier particles were added to the reactor. This corresponded to an unfluidized bed height of roughly 120 mm.

3.3 Experimental procedure

Natural gas with a composition equivalent to $C_{1.154}H_{4.255}O_{0.024}N_{0.007}$ was used as fuel. For stoichiometric combustion, the oxygen consumption was 2.21 moles of O_2 per mole natural gas while stoichiometric partial oxidation required 0.57 moles of O_2 per mole natural gas.

A reactor temperature between 820-930 °C was desired. Before the actual reforming experiment was started, the furnace was heated to 20-30 °C above the desired fuel reactor temperature. During the heating period the reactors were fluidized with air. When sufficiently high temperature was reached the air going to the fuel reactor was replaced by fuel. This initially resulted in chemical-looping combustion, but since the reactor system was operated at understoichiometric conditions and the oxygen added to the air reactor was insufficient to fully reoxidize the oxygen-carrier particles, steady-state conditions with chemical-looping reforming was gradually approached. This took 20-35 minutes, depending on the flows of air and fuel. The reason for the slow response is that in the beginning of each experiment the active phase of the oxygen carrier was fully oxidized to NiO. In order to reach steady-state conditions roughly 40% of available NiO needed to be reduced to Ni, and this took some time due to the relatively low fuel flow.

Reforming tests were performed both with dry fuel and fuel with extra steam added. The reason for adding steam to some of the experiments was twofold. Firstly, it was made to examine if it was possible to combine partial oxidation and steam reforming in the same reactor vessel, utilizing metallic Ni formed on the surface of the oxygen-carrier particles as steam reformer catalyst. Secondly, steam was added to see if it would affect formation of solid carbon, which could possibly occur in the fuel reactor. The periods of continuous reforming at stable conditions lasted from 70 minutes to 4 hours and 20 minutes. In total, 24 hours of reforming with dry natural gas and 17 hours with natural gas and steam were recorded.

For the experiments with steam, a mixture of 75 vol% natural gas and 25 vol% steam was desired. A higher steam concentration would likely result in increased H_2 yield, but high steam concentration in the fuel reactor would also mean that the overall reaction enthalpy of the reactor system would be endothermic due to reaction (11) which, unlike reaction (9) and reaction (10), does not provide any Ni to be oxidized with the exothermic reaction (8). A chemical-looping reforming process could be configured in many ways,

but a mix with 75 vol% natural gas and 25 vol% steam seems reasonable if a thermally balanced process is desired; see also Mattisson et al [8] and Rydén et al [9].

Steam was added by bubbling natural gas through hot water with a temperature of 90-95 °C. The gas mixture was then cooled to 66-68 °C in a cooling column and the resulting condensate was removed. The steam saturated gas was transferred to the reactor in a heated tube with a temperature of 120-130 °C. This resulted in a gas mixture consisting of 23-27 vol% H_2O and 73-77 vol% natural gas. So for most cases, the H_2O concentration in the fuel should have been close to 25 vol%. All calculations presented in this paper are based on this number.

The gas streams from the air reactor and the fuel reactor were analyzed individually. Before entering the analyzers they passed particle filters, coolers and water traps. Therefore, all measurements were made on dry gas. CO, CO_2 and CH_4 were measured using IR analyzers while O_2 was measured with paramagnetic sensors. In addition to this, the gas from the fuel reactor was examined with a chromatograph, a Varian Micro-GC CP4900 equipped with Molsieve 5A and PoraPLOT Q columns. The chromatograph was needed to measure H_2 and CO at high concentrations and it also measured CO_2 and CH_4.

On the exit pipe from the fuel reactor there was a water seal that made it possible to increase the pressure in the fuel reactor by altering the height of the water column. The column height was fixed to 20 mm which corresponds to an overpressure in the fuel reactor of 196 Pa. This was done to minimize the dilution of the fuel reactor gas.

The pressure was measured along the reactors. It was possible to approximately establish the amount of solids present in each reactor from the pressure difference between the measuring locations.

The slot and the downcomer were fluidized with minor amounts of Ar, corresponding to 0.2-0.3% of the total gas flow through the reactors. This was made to improve the particle circulation.

4. Results

Each continuous reformer test has been given a designation. Case 1D-6D is reforming of dry natural gas while case 7S-13S is reforming of natural gas with 25 vol% steam. These 13 cases were performed without parameter variations. A summary of the experimental conditions is shown in table 1.

Case	AR Air (l/min)	FR Fuel (l/min)	FR Steam (l/min)	Air ratio	Duration (min)	FR Temperature (°C)
1D	4.00	0.57	0	0.67	140	862-863
2D	4.00	0.64	0	0.60	140	901-907
3D	7.00	1.00	0	0.67	195	908-918
4D	6.00	0.95	0	0.60	140	915-921
5D	5.50	0.82	0	0.64	260	921-924
6D	5.50	0.78	0	0.67	190	921-925
7S	4.78	0.68	0.23	0.67	240	921-923
8S	4.29	0.68	0.23	0.60	225	918-921
9S	3.79	0.68	0.23	0.53	200	908-920
10S	5.50	0.99	0.33	0.53	110	888-914
11S	4.00	0.64	0.21	0.60	70	836-837
12S	4.00	0.72	0.24	0.53	70	831-833
13S	4.00	0.80	0.26	0.48	80	824-827

Table 1. Summary of the experimental conditions and gas flows for the air reactor (AR) and the fuel reactor (FR).

Prior to the experiments presented in table 1, six hours of chemical-looping reforming of dry natural gas with parameter variations was accomplished. These experiments worked well, but the transients made evaluation and interpretation of the results difficult, hence the data is not reported here.

In table 1, the air ratio indicates the amount of air that is added to the air reactor compared to what is required for stoichiometric combustion of the fuel added to the fuel reactor. Duration is the time period of uninterrupted reforming, after steady state has been reached. In general, the overall duration of each experiment was another hour or two due to start-up and shut-down procedures.

4.1 Reformer gas composition

In a gas reforming process H_2 and CO are the wanted products. Other gases that could be present after the fuel reactor include H_2O, CO_2, CH_4, N_2, O_2, Ar and higher hydrocarbons.

All measurements were made after that H_2O had been removed by condensation. In order to make evaluation of the experiments straightforward $x_{O2,dry}$ and $x_{CH4,dry}$ were set to zero during active reforming, where $x_{i,dry}$ is the volume fraction of component i in dry gas. This simplification can be justified since measured concentrations of CH_4 and O_2 during operation were below the detection limit. It was also assumed that the concentration of higher hydrocarbons was zero. This assumption seems reasonable since no higher

hydrocarbons were detected with the gas chromatograph. In addition to this, higher hydrocarbons are believed to be much more reactive with the oxygen carrier than CH_4. N_2 and Ar in the reformer gas originate from dilution with air from the air reactor and from the small amounts of Ar that was used for fluidization in the slot and downcomer. It was not possible to differentiate between these two inert gases so they were combined into $x_{N2,dry}$ which could be calculated as $1-x_{H2,dry}-x_{CO,dry}-x_{CO2,dry}$.

In general, the reforming experiments were successful. Complete conversion of fuel and high selectivity towards H_2 and CO were achieved for all cases. An example of the resulting gas composition for reforming of dry natural gas is shown in figure 4.

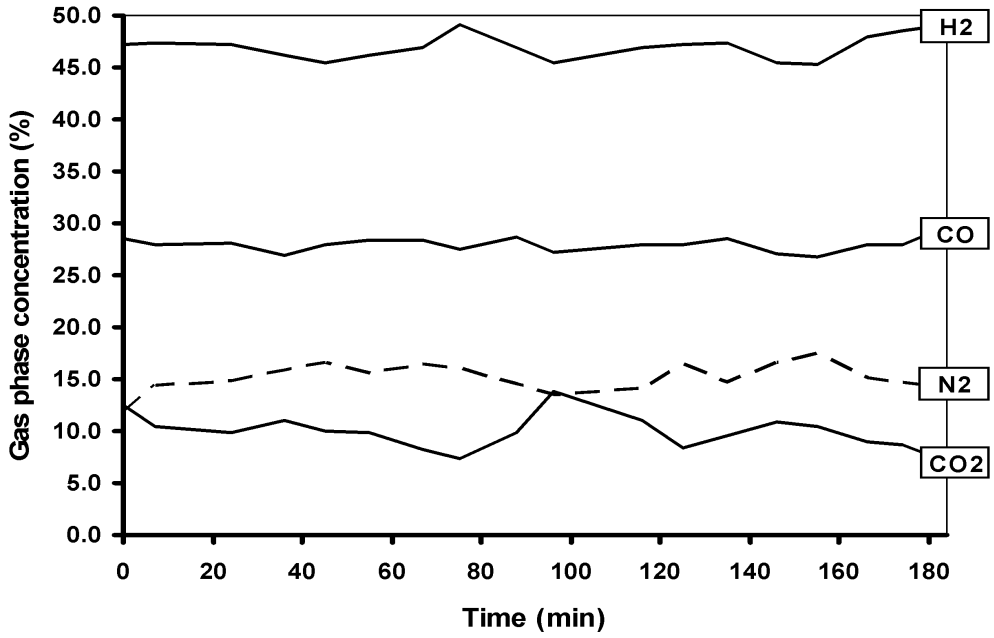

Figure 4. Dry gas composition after the fuel reactor as a function of time for case 3D.

An example of reforming of natural gas with 25 vol% steam is shown in figure 5. When compared to figure 4, it can be see that both examples show similar concentrations of CO and CO_2 while the H_2 concentration is higher for the experiment with steam. The H_2O concentration should also be higher in this case, but this can not be seen directly since all measurements were made on dry gas.

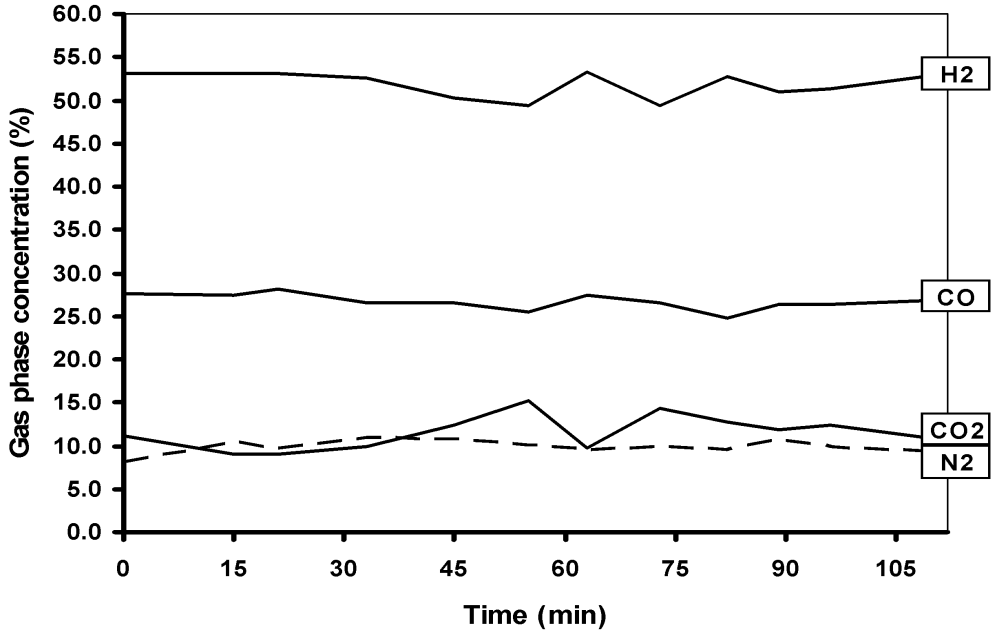

Figure 5. Dry gas composition after the fuel reactor as a function of time for case 10S.

The data presented in figure 4-6 are based on measurements with the chromatograph, so there is 7-10 minutes between each data point. It can be seen that the gas composition varied slightly during the experiments. The average gas composition for each case is presented in table 2, where the reported values for CO_2 and CO in the gas from the air reactor is due to leakages between the air reactor and the fuel reactor, see section 4.2-4.3 below for a discussion about this.

Case	AR $x_{CO2,dry}$ (average %)	AR $x_{CO,dry}$ (average %)	FR $x_{CO2,dry}$ (average %)	FR $x_{CO,dry}$ (average %)	FR $x_{H2,dry}$ (average %)
1D	5.9	0.2	13.6	26.7	50.5
2D	8.0	0.4	5.3	26.5	58.2
3D	6.1	0.2	9.9	28.0	47.0
4D	7.4	0.6	4.6	27.4	53.4
5D	8.0	0.4	7.9	29.6	53.0
6D	7.4	0.3	11.4	26.7	51.5
7S	6.4	0.3	16.9	25.7	48.3
8S	6.3	0.5	11.2	26.6	54.3
9S	4.2	0.8	11.0	26.7	52.2
10S	4.3	1.8	11.5	26.7	51.8
11S	3.9	1.7	21.7	23.2	49.4
12S	4.0	1.8	15.5	24.5	51.7
13S	4.2	4.8	10.9	25.8	55.1

Table 2. Measured dry gas composition for the air reactor (AR) and for the fuel reactor (FR).

4.2 Formation of solid carbon in the fuel reactor

As mentioned earlier all measurements were made on dry gas. If it was assumed that there was no formation of solid carbon in the fuel reactor, the actual composition of the reformer gas including H_2O could be estimated by a species balance. Under this assumption the ratio (H/C) remains the same in the reformer gas as it was in the fuel, see expression (13).

$$(H/C)_{\text{fuel mix}} = (H/C)_{\text{reformer gas}} \quad (13)$$

For natural gas with the composition C_nH_m, with or without extra steam, $(H/C)_{\text{fuel mix}}$ can be calculated with expression (14), where $x_{H2O,fuel}$ is the volume fraction steam.

$$(H/C)_{\text{fuel mix}} = [\,(1 - x_{H2O,fuel}) \times m + x_{H2O,fuel} \times 2\,] \,/\, [\,(1 - x_{H2O,fuel}) \times n\,] \quad (14)$$

If $y_{i,sb}$ is set to $x_{i,dry}$ for CO_2, CO and H_2, a corresponding value $y_{H2O,sb}$ is obtained from expression (15), and the gas composition including H_2O can be calculated with expression (16), where $x_{i,sb}$ is the volume fraction of component i according to the species balance (sb).

$$(H/C)_{\text{reformer gas}} = [\,y_{H2O,sb} \times 2 + y_{H2,sb} \times 2\,] \,/\, [\,y_{CO2,sb} + y_{CO,sb}\,] \quad (15)$$

$$x_{i,sb} = y_{i,sb} \,/\, (\,y_{CO2,sb} + y_{CO,sb} + y_{H2,sb} + y_{H2O,sb}\,) \quad (16)$$

When the reformer gas composition was calculated from expressions (13-16), it was found that the obtained values for $x_{H2O,sb}$ did not always correspond to the expected. At extreme occasions calculated $x_{H2O,sb}$ became very low or even negative, see figure 6 for an example. It is believed that this phenomenon was due to formation of solid carbon in the fuel reactor.

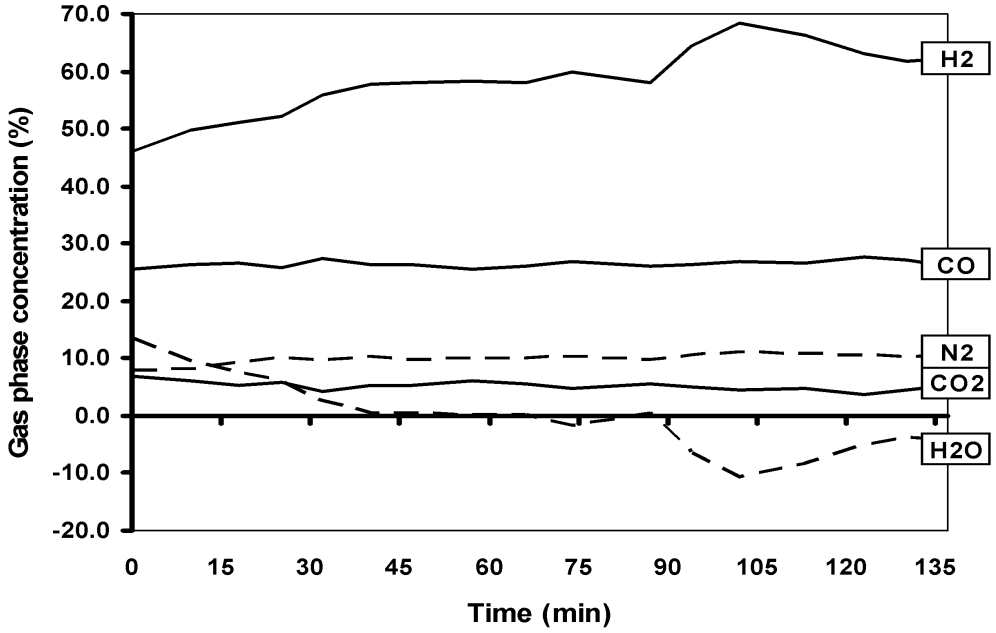

Figure 6. Gas composition including H_2O after the fuel reactor as a function of time for case 2D, when H_2O is calculated according to expressions (13-16).

Formation of solid carbon would mean that the hydrogen content of the fuel is released as usual, while the carbon could either be accumulated in the fuel reactor or transferred to the air reactor via the particle circulation, where it most likely would burn with air. This means that $(H/C)_{\text{reformer gas}}$ increases and becomes higher than $(H/C)_{\text{fuel mix}}$. Hence, the H_2O concentration calculated with expressions (13-16) becomes inaccurate.

Solid carbon could be formed either through the Boudouard reaction, reaction (17), or through various kinds of hydrocarbon decomposition, reaction (18).

Boudouard reaction:	$2CO \rightarrow C + CO_2$	(17)
Hydrocarbon decomposition:	$C_nH_m \rightarrow nC + (½m)H_2$	(18)

Carbon formation is a phenomenon that is known from other reforming processes, and since reactions (17-18) are catalysed by metallic Ni it is not surprising that it could occur during chemical-looping reforming.

Carbon formation on oxygen-carrier particles for chemical-looping combustion has been examined by Cho et al [17]. A single fluidized-bed reactor was used and chemical-looping was simulated by alternating between reduction and oxidation. Particles of $NiO/NiAl_2O_4$ and Fe_2O_3/Al_2O_3 were used as oxygen carrier and the reactor temperature was 750-950 °C. It was found that carbon formation on Ni-based particles was strongly dependent on the availability of oxygen. When more than 80% of available NiO was reduced to Ni the formation of solid carbon was rapid. Adding 50 vol% steam to the fuel

seemed to hamper carbon formation under some circumstances. In the study presented in this paper, it is estimated that only about 40% of available NiO was reduced to Ni during operation, see section 4.5 below. The study by Cho et al [17] suggests that this degree of reduction should not result in any extensive carbon formation.

The experimental setup did not allow carbon formation to be measured directly, but it was possible to make estimations. The assumption that needs to be made is that the water-gas shift reaction is at thermodynamical equilibrium after the fuel reactor. This seems reasonable since the temperature in the fuel reactor is high and reaction (4) is known to be fast. Under this assumption, and if $y_{i,td}$ is set to $x_{i,dry}$ for CO_2, CO and H_2, a corresponding value $y_{H2O,td}$ is obtained from expression (19), and the gas composition including H_2O can be calculated with expression (20), where $x_{i,td}$ is the volume fraction of component i and $K_{c,td}$ is the equilibrium constant for reaction (4), which is dependent on the temperature and can be calculated from thermodynamical data (td).

$$K_{c,td} = [\, y_{CO2,td} \times y_{H2,td} \,] \,/\, [\, y_{CO,td} \times y_{H2O,td} \,] \tag{19}$$

$$x_{i,td} = y_{i,td} \,/\, (\, y_{CO2,td} + y_{CO,td} + y_{H2,td} + y_{H2O,td} \,) \tag{20}$$

To make it easy to compare how well the gas composition obtained with expressions (19-20) corresponds to the one obtained with expressions (13-16) a quota $Q_{c,sb}$ is defined:

$$Q_{c,sb} = [\, x_{CO2,sb} \times x_{H2,sb} \,] \,/\, [\, x_{CO,sb} \times x_{H2O,sb} \,] \tag{21}$$

It should be pointed out that $K_{c,td}$ and $Q_{c,sb}$ are different. Expression (19) is always valid if the gas mixture is at thermodynamical equilibrium, while expression (21) describes the relation between the gas components in the reformer gas for a particular case under the assumption that there is no formation of solid carbon. If $(Q_{c,sb}/K_{c,td}) = 1$ the reformer gas is at thermodynamical equilibrium and there is no formation of solid carbon.

If $(H/C)_{fuel\ mix}$ is calculated with expression (14) and it is assumed that the reformer gas is at thermodynamical equilibrium, expressions (22) can be used to calculate the level of carbon formation, C_{td}.

$$(H/C)_{fuel\ mix} = [\, x_{H2,td} \times 2 + x_{H2O,td} \times 2 \,] \,/\, [\, x_{CO,td} + x_{CO2,td} + C_{td} \,] \tag{22}$$

The formation of solid carbon expressed as a fraction of added carbon, C(s) can be calculated with expression (23).

$$C(s) = C_{td} \,/\, [\, C_{td} + x_{CO,td} + x_{CO2,td} \,] \tag{23}$$

Values for C(s) and $(Q_{c,sb}/K_{c,td})$ for each case are presented in table 3 below. These numbers could be seen as indicators for when substantial carbon formation occur.

Another way to examine carbon formation is to study if there was carbon accumulated in the reactors during operation. After a reformer experiment was finished, fuel and air was replaced by N_2 for a short period of time. Then air was added to the reactors. If this resulted in detectable CO_2 it should be a result of carbon accumulation in the reactors. The carbon accumulation could be estimated by integrating the area under the CO_2 curves, see figure 7 for an example.

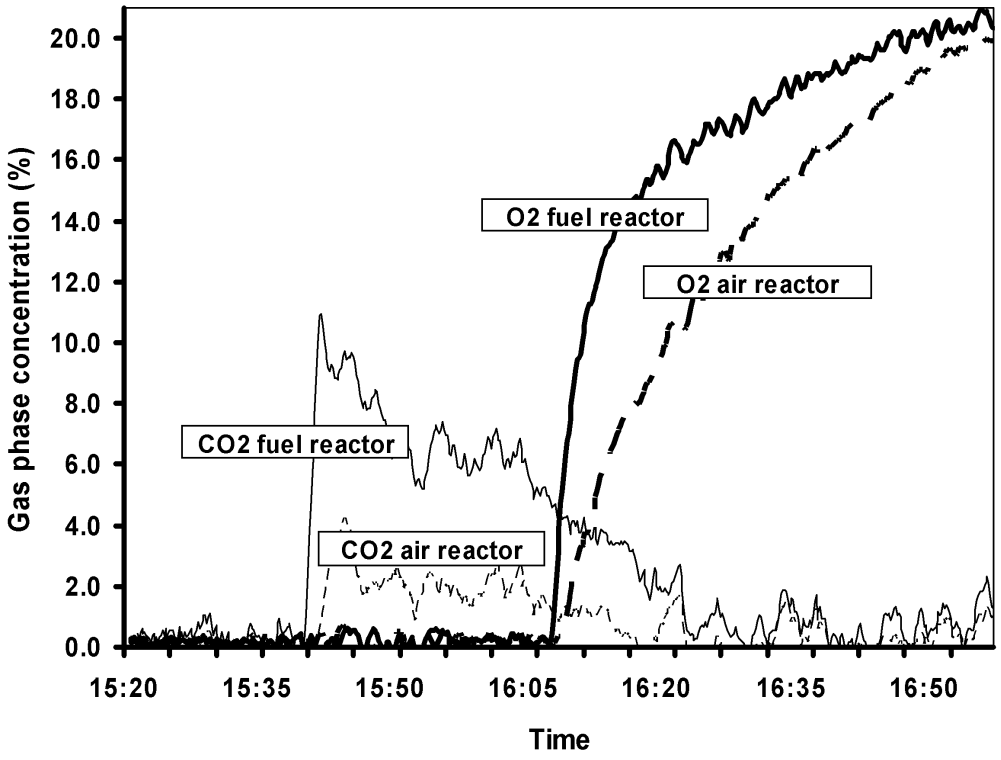

Figure 7. Plot for estimation of carbon accumulation and the degree of NiO reduction for case 6D.

In figure 7, accumulated carbon is burned off with 1 l/min air in each reactor part, starting at 15:40. It can be seen that there is CO_2 emitted also from the air reactor. This is most likely due to gas leakages from the fuel reactor. The fact that there is a correlation between the CO_2 concentration after the air and fuel reactor, in figure 7 as well as in other cases, supports this hypothesis.

Of the experiments with dry natural gas, case 3D was almost free from carbon accumulation. For the other cases between 0.6 and 2.6% of the total amounts of carbon added with the fuel was accumulated in the reactor system as solid carbon. For most tests with natural gas with steam no carbon accumulation could be detected. However, for case

9S the carbon accumulation was estimated to be 0.3%. A summary of the estimated carbon accumulations for each reformer case can be found in table 3.

Case	($Q_{c,sb}$ / $K_{c,td}$)	C(s) estimated (average %)	C(s) accumulated (%)
1D	0.79	7.7	No data
2D	0.00	19.9	≈2.6
3D	1.02	-0.7	≈0.1
4D	0.42	10.1	≈0.6
5D	0.75	5.0	≈1.6
6D	0.61	14.3	≈1.8
7S	0.98	1.3	≈0.3
8S	0.88	4.2	0
9S	0.98	0.9	0
10S	1.03	-0.7	0
11S	0.94	3.0	0
12S	0.97	1.3	0
13S	0.98	0.9	0

Table 3. Carbon accumulation and estimated carbon formation for each reformer case.

The interpretation of the data in table 3 is somewhat uncertain. Carbon formation seems to have been small for reforming with natural gas with steam and for case 5D with dry fuel. For these cases the composition of the fuel reactor gas was close to thermodynamical equilibrium and there was little or no detectable carbon accumulation. For the remaining cases with reforming of dry natural gas the resulting gas composition differed considerably from equilibrium and solid carbon was accumulated in the reactors.

Carbon formation could occur both on the surface of the oxygen-carrier particles or elsewhere in the fuel reactor. Carbon formation directly on the particles seems likely due to the catalytic properties of Ni. If this happened the formed carbon should not be accumulated in the reactor system, but follow the particle circulation to the air reactor and burn there. Unfortunately, the used experimental setup did not make it possible to quantify this type of carbon formation directly.

The oxidation and reduction behaviour of oxygen-carrier particles made of $NiO/MgAl_2O_4$ have been examined by Mattisson et al [16]. A single fluidised bed reactor was used and chemical-looping was simulated by switching between a reduction period with a mixture of 50% CH_4 and 50% H_2O, an inert period with N_2, and a oxidation period with a mixture of 5% O_2 and 95% N_2. The reactor temperature was 950 °C, and it is reported that when carbon was formed on the surface of the oxygen-carrier particles it reacted with NiO and formed CO in a solid-phase reaction during the inert period. No such phenomenon was observed during in the study described in this paper. This could be seen as an indication that there was no carbon formation on the surface of the oxygen-

carrier particles. It shall be noticed however, that the reactor temperature was lower in the study presented in this paper.

In the study by Mattisson et al [16], it was also found that solid carbon on the surface of $NiO/MgAl_2O_4$ particles was oxidized almost immediately when the oxidation period started. No such phenomenon was observer in the study presented in this paper. On the contrary, in figure 7 it can be seen that combustion of accumulated carbon was slow. There was still carbon left in the reactor system after 30 minutes, when most of the Ni had been oxidized and the O_2 concentration had started to increase. This suggests that the accumulated carbon was not located on the surface of the oxygen-carrier particles but somewhere where it was prevented from direct oxidation with air.

The most likely location for carbon accumulation is the pressure measurement taps connected to the lower part of the fuel reactor. The inlets of these taps are stagnant zones with temperatures well over 800 °C, which are conditions that could result in thermal decomposition of hydrocarbons via reaction (18). This hypothesis is supported by the fact that black substance was observed in the plastic tubes leading to the taps.

In table 3, it can be seen that the carbon accumulation often differs from the estimated carbon formation. There are two possible explanations for this. Firstly, it is possible that the reformer gas was not at thermodynamical equilibrium. Hence, the calculated value for carbon formations becomes inaccurate. Secondly, solid carbon could have followed the particle circulation to the air reactor and burnt there. The relative importance of these factors is not known.

4.3 Leakage between the air reactor and the fuel reactor

In figure 4-6, it can be seen that the reformer gas was diluted with N_2. The dilution varied, but for most cases $x_{(N2)}$ was 7-15% measured on dry gas. In table 2 it can be seen that there was CO_2 and sometimes also CO present after the air reactor. Both these effects should be due to gas leakage between the reactors, most likely through the slot and maybe also through the downcomer. CO_2 and CO after the air reactor could also be a result of carbon formation in the fuel reactor.

It is possible to estimate the leakage between the reactors with a simple species balance. Estimations of the average leakage can be found in table 4. The N_2 in the natural gas and the Ar that is used to fluidize the slot and downcomer can be neglected. Carbon formation in the fuel reactor would have very little impact on the numbers in table 4, and have not been considered.

Case	AR to FR N_2 leakage (average %)	FR to AR C_x leakage (average %)
1D	1.5	30.7
2D	1.6	38.3
3D	2.6	31.2
4D	2.6	36.4
5D	1.4	41.1
6D	1.5	39.5
7S	1.4	34.0
8S	1.4	31.1
9S	2.4	19.8
10S	2.3	24.2
11S	1.1	24.9
12S	1.8	22.9
13S	1.9	33.3

Table 4. Average gas leakage for each case.

In table 4, it can be seen that roughly 1-3% of the N_2 added with air in the air reactor leaked to the fuel reactor. Hence it is possible that a small share of the reformer products was formed with O_2 from leaking air rather than with oxygen from NiO and H_2O. The size of this leakage suggests that this should not have much impact on the overall results. It can also be seen that the corresponding leakage from the fuel reactor to the air reactor was much bigger. In the order of 20-40% of the carbon added to the fuel reactor ended up in the air reactor. The main reason for this should be gas leakage due to the elevated pressure in the fuel reactor. It is also possible that solid carbon was formed on the oxygen-carrier particles in the fuel reactor, followed the particle circulation to the air reactor and burned there, as is described in section 4.2 above.

It should be pointed out that the gas leakages between the air reactor and fuel reactor reported in this paper are a consequence of the simplified reactor design. In a real-world system gas leakage between the reactors could easily be eliminated, for example by introducing fluidized particle-gas locks between the reactor vessels. This has been demonstrated by Lyngfelt et al in a 10 kW chemical-looping combustion reactor [11].

4.4 Oxygen ratio

In table 3, it can be seen that the reformer gas composition is close to thermodynamical equilibrium for all tests with natural gas mixed with steam, as well as for case 3D with dry natural gas. This can be illustrated by plotting the calculated gas composition in an equilibrium diagram, see figure 8 for an example.

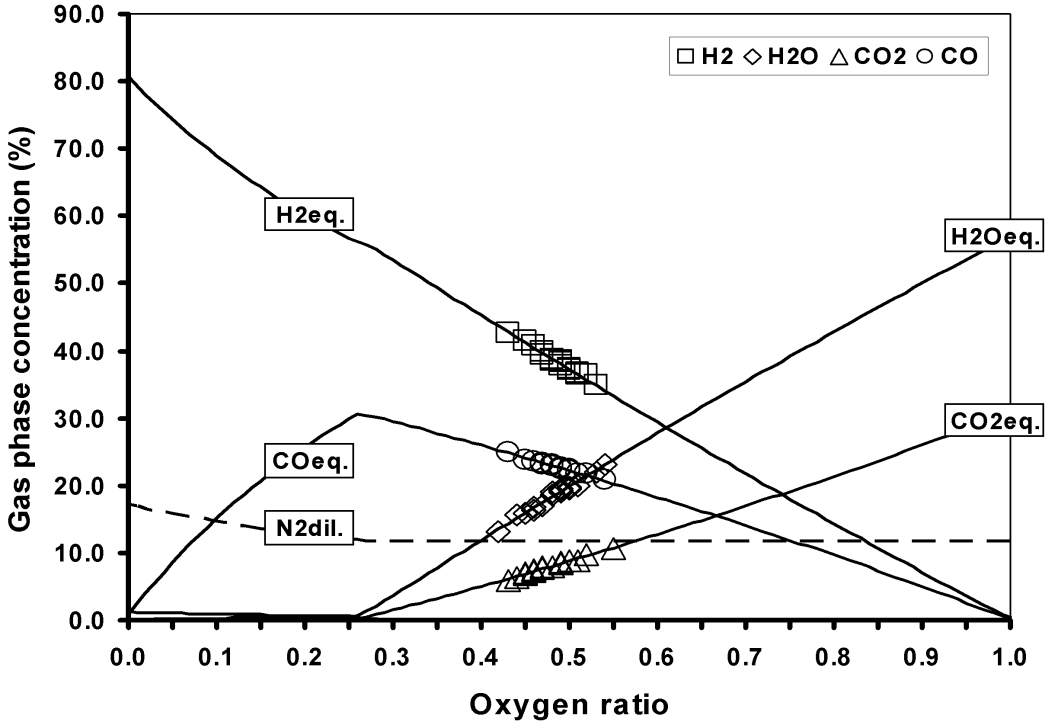

Figure 8. Data according to expressions (13-16) for case 3D compared to thermodynamical equilibrium for chemical-looping reforming of natural gas at 920 °C with 12% N_2 dilution.

In figure 8, the oxygen ratio is defined as the amount of oxygen that is reacting with the fuel compared to what is needed for combustion. An oxygen ratio of 1.0 corresponds to complete conversion of the fuel to H_2O and CO_2. Since combustion of 1 mole of the natural gas required 2.21 moles O_2, an oxygen ratio of 1.0 corresponds to $2 \times 2.21 = 4.42$ moles reacted NiO per mole natural gas. In comparison, with an oxygen ratio of 0.26 there is just enough oxygen available to reform the fuel to H_2 and CO. This corresponds to $0.26 \times 4.42 = 1.15$ moles reacted NiO.

In figure 8, it can be seen that the reformer gas composition during the test corresponds to thermodynamical equilibrium with an oxygen ratio of 0.43-0.54. In table 1, it can be seen that the corresponding air ratio is 0.67. The reason for this difference should be the leakage from the fuel reactor to the air reactor, mentioned in section 4.3 above. In the air reactor leaking natural gas, H_2 and CO burns to CO_2 and H_2O and thus consumes extra O_2. Consequently, less NiO is produced and delivered to the fuel reactor than what the air ratio is indicating. If solid carbon is formed in the fuel reactor and transferred to the air reactor via the particle circulation it would burn there and contribute to a reduced oxygen factor as well.

The oxygen ratio could be estimated by comparing the (O/C) ratio for the reformer gas with the (O/C) ratio for complete oxidation of the fuel. In order to do so the

reformer gas composition including H_2O is required. Hence two estimations was obtained, since the (O/C) ratio for the reformer gas could be calculated either by assuming that there was no carbon formation using the gas composition obtained by expressions (13-16), or by assuming that the water-gas shift reaction was at thermodynamic equilibrium using the gas composition obtained by expressions (19-20). The oxygen ratio could also be estimated from the gas leakage between the reactors. In order to do so it was assumed that the gas leakage from the fuel reactor to the air reactor, reported in table 4, had the same composition as the reformer gas calculated with expressions (13-16). It was also assumed that H_2 and CO in the leaking gas reacted with O_2 in the air reactor, forming CO_2 and H_2O until thermodynamical equilibrium was reached. Thus the oxygen ratio could be estimated by subtracting the extra O_2 consumed in the air reactor from the O_2 added with the air. Estimations for the average oxygen ratio using these methods can be found in see table 5.

Case	Air ratio (added to reactors)	Oxygen ratio (expressions 13-16)	Oxygen ratio (expressions 19-20)	Oxygen ratio (from average gas leakage)
1D	0.67	0.50	0.54	0.53
2D	0.60	0.30	0.42	0.37
3D	0.67	0.48	0.48	0.52
4D	0.60	0.34	0.39	0.41
5D	0.64	0.41	0.44	0.44
6D	0.67	0.46	0.54	0.48
7S	0.67	0.54	0.55	0.53
8S	0.60	0.44	0.46	0.46
9S	0.53	0.45	0.46	0.46
10S	0.53	0.46	0.46	0.48
11S	0.60	0.58	0.59	0.56
12S	0.53	0.50	0.51	0.48
13S	0.48	0.42	0.43	0.45

Table 5. Air ratio compared to oxygen ratio.

In table 5, it can be seen that the oxygen ratio seems to have been in the order of 0.40-0.50 for most experiments. It should be noticed that the numbers are uncertain for the cases when carbon formation is believed to be significant. For the experiments with natural gas with 25 vol% steam the estimations are much more consistent.

If compared to the numbers from table 3, it can be seen that there might be a correlation between low oxygen ratio and carbon formation, at least when dry natural gas is used as fuel. Although the picture is not clear it seems reasonable to believe that carbon formation is more likely to occur at low oxygen ratios than at higher ones.

4.5 Effects on the oxygen-carrier particles

After the experiments were finished the reactor was opened and the oxygen carrier particles examined. It was found that some of the particles in the air reactor had formed lumps with a diameter of up to 20 mm. The lumps were soft and only a small force was needed to break them apart. Despite the lumps, the oxygen-carrier particles were never deactivated and it was still possible to perform successful reforming.

There was 315 g of oxygen carrier left in the reactors so the loss during operation was 35 g. The lost particles were blown through the fuel reactor the first time the pressure measurement taps were cleaned, which was done by back blowing with pressurized N_2. The lost particles were found in the water trap after the reactor system. After this accident the loss of particles was minimal.

The degree of oxidation of the oxygen-carrier particles was estimated as is shown in figure 7 above, where 1 l/min air is fed to each reactor starting at 15:40. The amount of O_2 needed to oxidize the reduced oxygen carrier is the area above the O_2 curves minus the area under the CO_2 curves. It was found that 33-44% of the available NiO was reduced to Ni during operation. At this point steady state was achieved and the remaining NiO was not reduced.

5. Discussion

The experiments described in this paper demonstrate that chemical-looping reforming is a feasible concept. Complete conversion of natural gas and good selectivity towards the desired products was achieved. It was also shown that it is possible to have partial oxidation and steam reforming simultaneously in the fuel reactor. The oxygen ratio, which is the amount of oxygen carrier that has reacted with the fuel compared to what is required for complete conversion to CO_2 and H_2O, was in the range of 0.4 to 0.5 in most of the experiments. The reactor was operating at atmospheric pressure and at temperatures between 820 °C and 930 °C.

The experimental conditions are not directly emulating those of future industrial processes. On the contrary, it is clear that different process conditions will be attractive for most real world applications. Firstly, it shall be pointed out that reforming of hydrocarbons leads to a large volumetric increase, see reactions (1-3). Therefore, the power required for compression of produced H_2 or synthesis gas to suitable product pressure would be considerable for any process working at atmospheric pressure. As a consequence, elevated pressure during the reforming would be highly beneficial for the process economy. Elevated pressure would probably make reactor temperatures of 1000 °C or higher necessary, in order to obtain sufficient conversion of the fuel. Secondly, a

different oxygen ratio may be wanted. A low oxygen ratio could be used to maximize the amount of produced H_2 and CO while a higher oxygen ratio would be attractive if a process for cogeneration of H_2, power and heat is wanted.

The results of the experiments indicate that carbon formation should be no problem if some steam is added to the fuel. For reforming of dry natural gas there seems to have been quite significant carbon formation at some occasions. It is not clear if this was an effect of carbon formation on the oxygen-carrier particles or if it is was due to reactor design, such as carbon formation in stagnant zones or in the pressure measurement taps. Carbon formation during chemical-looping reforming should be examined further, using experimental setups that provide good opportunities to study the phenomenon in detail.

It should be noticed that carbon formation might not necessarily be a big problem. If the carbon follows the oxygen-carrier particles to the air reactor it would burn there and release heat that could be used for the endothermic reformer reactions in the fuel reactor. This would dilute the N_2 from the air reactor with CO_2 though, so if chemical-looping reforming is to be utilized for production of synthesis gas or H_2 with CO_2 capture carbon formation would lead to reduced capture efficiency.

As mentioned above, the oxygen carrier particles formed soft lumps in the air reactor. It seems likely that the formation of lumps can be explained by the low fluidization velocities used. During reforming the superficial gas velocity in the air reactor was in the order of 0.5 m/s, and it was only 0.1 m/s during combustion of accumulated carbon and reoxidation of the oxygen-carrier particles. This should be compared to the expected superficial gas velocity in a real-world riser which is at least 5 m/s. It seems unlikely that the lumps would have formed and survived at these velocities. After 41 h of chemical-looping reforming, several hours of chemical-looping combustion and additional operation without fuel, the particles had not formed any hard agglomerates. This suggests that the tendency for forming hard agglomerates is low. Nevertheless, the phenomenon should be examined further since stable and durable oxygen-carrier particles will be crucial for any practical chemical-looping reforming application.

Although the oxygen-carrier particles used worked well, other active phases than NiO should be examined. Mixtures of NiO and other metal oxides should also be considered, as well as different inert phases. The goal should be to find a cheap, long lasting and environmentally sound oxygen carrier with good reactivity and high selectivity towards CO and H_2. NiO seems to be most effective active phase but there might be other alternatives as well. In the study by Ishida et al [10], it is reported that carbon formation on the particle surface was much lower for CoO and CoO/NiO than for NiO. Such particles could prove to be attractive for chemical-looping reforming.

6. Conclusions

Chemical-looping reforming has been demonstrated in a continuous laboratory reactor consisting of two interconnected fluidized beds. Natural gas has been used as fuel. The oxygen carrier was made of NiO and $MgAl_2O_4$. In some tests 25 vol% steam was added to the natural gas. The reformer temperature was in the interval 820-930 °C. Complete conversion of natural gas was achieved and the selectivity towards H_2 and CO was good. Formation of solid carbon was identified as a potential problem and was apparent for some of the experiments with dry natural gas. For most experiments with natural gas and 25 vol% steam there was no accumulation of carbon in the reactors and the composition of the reformer gas was close to thermodynamical equilibrium, which indicates that the carbon formation was very low. The experiments confirm that the concept chemical-looping reforming is feasible and should be further investigated.

7. Acknowledgements

The authors wish to thank our supporters and financers, the Nordic CO_2 Sequestration Program ($NoCO_2$), the Swedish Gas Centre (SGC), the National Swedish Energy Agency (STEM) and Ångpanneföreningen's Foundation for Research and Development. The authors also wish to thank Dr. Eva Johansson who designed the laboratory reactor that was used for the study.

8. References

[1] Cho P. Development and characterization of oxygen-carrier materials for chemical-looping combustion. Doctoral thesis, Chalmers University of Technology, Göteborg, Sweden, 2005.
[2] Johansson M. Selection of oxygen carriers for chemical-looping combustion using methane as fuel. Licentiate thesis, Chalmers University of Technology, Göteborg, Sweden, 2005.
[3] Adánez J, De Diego LF, García-Labiano F, Gayán P, Abad A. Selection of oxygen carriers for chemical-looping combustion. Energy & Fuels 2003;18:371-377.
[4] Mattisson T, Lyngfelt A. Applications of chemical-looping combustion with capture of CO_2. Proceedings of the Second Nordic Minisymposium on Carbon Dioxide Capture and Storage, Göteborg, Sweden, 2001.
[5] Stobbe ER, De Boer BA, Geus JW. The reduction and oxidation behaviour of manganese oxides. Catalysis Today 1999;47:161-167.

[6] Fathi M, Bjorgum E, Viig T, Rokstad OA. Partial oxidation of methane to synthesis gas: Elimination of gas phase oxygen. Catalysis Today 2000;63:489-497.
[7] Zafar Q, Mattisson T, Gevert B. Integrated hydrogen and power production with CO_2 capture using chemical-looping reforming - redox reactivity of particles of CuO, Mn_2O_3, NiO, and Fe_2O_3 using SiO_2 as a support. Industrial & Engineering Chemistry Research 2005;44:3485-3498.
[8] Mattisson T, Zafar Q, Lyngfelt A, Gevert B. Integrated hydrogen and power production from natural gas with CO_2 capture. Proceedings of the 15th World Hydrogen Energy Conference, Yokohama, Japan, 2004.
[9] Rydén M, Lyngfelt A. Hydrogen and power production with integrated carbon dioxide capture by chemical-looping reforming. Proceedings of the 7th International Conference on Greenhouse Gas Control Technologies, Vancouver, Canada, September 2004.
[10] Ishida M, Jin H, Okamoto T. Development of a novel chemical-looping combustion: synthesis of a looping material with double metal oxide of CoO-NiO. Energy & Fuels 1998;12:1272-1277.
[11] Lyngfelt A, Kronberger B, Adánez J, Morin JX, Hurst P. The GRACE project. Development of oxygen carrier particles for chemical-looping combustion. Design and operation of a 10 kW chemical-looping combustor. Proceedings of the 7th International Conference on Greenhouse Gas Control Technologies, Vancouver, Canada, September 2004.
[12] Ryu HJ, Jin GT, Yi CK. Demonstration of inherent CO_2 separation and no NO_X emission in a 50 kW chemical-looping combustor: Continuous reduction and oxidation experiment. Poster presented at the 7th International Conference on Greenhouse Gas Control Technologies, Vancouver, Canada, September 2004.
[13] Johansson E. Fluidized-bed reactor systems for chemical-looping combustion with inherent CO_2 capture. Doctoral thesis, Chalmers University of Technology, Göteborg, Sweden, 2005.
[14] Abad A, Mattisson T, Lyngfelt A, Rydén M. Chemical-looping combustion in a 300 W continuously operating reactor system using a manganese-based oxygen carrier. Accepted for publication in Fuel.
[15] Kronberger B, Johansson E, Löffler G, Mattisson T, Lyngfelt A, Hofbauer H. A two-compartment fluidized bed reactor for CO_2 capture by chemical-looping combustion. Chemical Engineering and Technology 2004;27:1318-1326.
[16] Mattisson T, Johansson M, Lyngelt A. The use of NiO as an oxygen carrier in chemical-looping combustion. Fuel, in press 2005.
[17] Cho P, Mattisson T, Lyngfelt A. Carbon formation on nickel and iron oxide-containing oxygen carriers for chemical-looping combustion. Industrial & Engineering Chemistry Research 2005;44:668-676.